



Published in final edited form as:

J Biomech. 2016 June 14; 49(9): 1447–1453. doi:10.1016/j.jbiomech.2016.03.016.

Mechanical heterogeneities in the subendothelial matrix develop with age and decrease with exercise

Julie C. Kohn¹, Adeline Chen¹, Stephanie Cheng¹, Daniel R. Kowal², Michael R. King¹, and Cynthia A. Reinhart-King¹

¹Nancy E. and Peter C. Meinig School of Biomedical Engineering, Cornell University, Ithaca, NY 14853

²Department of Statistical Sciences, Cornell University, Ithaca, NY 14853

Abstract

Arterial stiffening occurs with age and is associated with lack of exercise. Notably both age and lack of exercise are major cardiovascular risk factors. While it is well established that bulk arterial stiffness increases with age, more recent data suggest that the intima, the innermost arterial layer, also stiffens during aging. Micro-scale mechanical characterization of individual layers is important because cells primarily sense the matrix that they are in contact with and not necessarily the bulk stiffness of the vessel wall. To investigate the relationship between age, exercise, and subendothelial matrix stiffening, atomic force microscopy was utilized here to indent the subendothelial matrix of the thoracic aorta from young, aged-sedentary, and aged-exercised mice, and elastic modulus values were compared to conventional pulse wave velocity measurements. The subendothelial matrix elastic modulus was elevated in aged-sedentary mice compared to young or aged-exercised mice, and the macro-scale stiffness of the artery was found to linearly correlate with the subendothelial matrix elastic modulus. Notably, we also found that with age, there exists an increase in the point-to-point variations in modulus across the subendothelial matrix, indicating non-uniform stiffening. Importantly, this heterogeneity is reversible with exercise. Given that vessel stiffening is known to cause aberrant endothelial cell behavior, and the spatial heterogeneities we find exist on a length scale much smaller than the size of a cell, these data suggest that further investigation in the heterogeneity of the subendothelial matrix elastic modulus is necessary to fully understand the effects of physiological matrix stiffening on cell function.

Keywords

atherosclerosis; stiffness; pulse wave velocity; atomic force microscopy; mechanotransduction

Corresponding Author: Cynthia A. Reinhart-King, 302 Weill Hall, 526 Campus Road, Ithaca, NY 14853, Phone: (607) 255-8491, Fax: (607) 255-7330, ; Email: cak57@cornell.edu

Conflict of interest statement

There are no conflicts of interest to state.

Publisher's Disclaimer: This is a PDF file of an unedited manuscript that has been accepted for publication. As a service to our customers we are providing this early version of the manuscript. The manuscript will undergo copyediting, typesetting, and review of the resulting proof before it is published in its final citable form. Please note that during the production process errors may be discovered which could affect the content, and all legal disclaimers that apply to the journal pertain.

Introduction

Risk factors for the development of cardiovascular disease (CVD) include increased age and lack of exercise (Grundy *et al.*, 1999), and risk is assessed clinically using macro-scale mechanical measurements. The standard clinical methodology to measure vessel stiffness and predict CVD is pulse wave velocity (PWV) testing, which is typically performed using ultrasound (Kohn and Lampi *et al.*, 2015; Laurent *et al.*, 2006; Mitchell *et al.*, 2010; Van Bortel *et al.*, 2012). PWV values have been shown to increase with age and decrease with exercise (Di Lascio *et al.*, 2014; Gu *et al.*, 2014a; Stepan *et al.*, 2014). However, while PWV is important in the prediction of the development of CVD, it is an indirect measure of bulk vessel stiffness and many studies attribute bulk mechanical properties to the medial layer (Kohn and Lampi *et al.*, 2015; Shadwick, 1999). Therefore, PWV does not provide information on the mechanical properties of individual layers of the blood vessel or measurements at a scale at which cells sense. Cells are known to respond to matrix stiffness (Kohn and Zhou *et al.*, 2015; Lo *et al.*, 2000) and their response to stiffening has been linked to vessel permeability and leukocyte transmigration (Huynh *et al.*, 2011; Krishnan *et al.*, 2011; Stroka and Aranda-Espinoza *et al.*, 2011a), hallmarks of atherosclerosis. Therefore, micro-scale elastic modulus measurement is necessary since macro-scale mechanical measurements do not provide a complete picture of subendothelial mechanics.

To measure the micro-scale properties of tissues, measurement techniques such as atomic force microscopy (AFM) have been implemented to probe the individual layers of the artery at the sub-micron level (Engler *et al.*, 2004; Klein *et al.*, 2009; Peloquin *et al.*, 2011). Previously, we used AFM to demonstrate that intimal arterial extracellular matrix (ECM) stiffness increases with age (Huynh *et al.*, 2011) and due to a high fat, high sugar diet (Weisbrod *et al.*, 2013). However, these studies focused on the mean mechanics of the subendothelial matrix and did not account for the complex spatial heterogeneities within the artery. Based on these and other similar studies, the predominant *in vitro* models used to study endothelial cell (EC) response to stiffness use primarily gels of homogeneous stiffness (Kohn and Zhou *et al.*, 2015; Klein *et al.*, 2009; Krishnan *et al.*, 2011; Stroka *et al.*, 2012; Wang and Pelham, 1998). However, cells are known to respond to heterogeneous matrix cues and display heterogeneous traction forces (Breckenridge *et al.*, 2014). The artery is a complex mechanical environment, and therefore we propose that the subendothelial matrix will display heterogeneous mechanical profiles, and that measuring these potential heterogeneities with respect to cardiovascular risk factors will allow us to better understand the mechanical environment ECs face *in vivo*.

Here, we characterize the mechanical variations in the elastic modulus of the subendothelial matrix as a function of age and exercise, two critical factors that affect the progression of atherosclerosis (Huynh *et al.*, 2011; Kohn and Lampi *et al.*, 2015; Tanaka *et al.*, 2000; Weisbrod *et al.*, 2013, Grundy *et al.*, 1999). Our data indicate that increased vessel stiffening with age is accompanied by an increase in spatial heterogeneities in elastic modulus, and exercise decreases this heterogeneity.

Methods

Animal Groups

All animal treatments and experiments were carried out under Cornell University's Institutional Animal Care and Use Committee guidelines. C57Bl/6 (B6) male mice were obtained from the National Institute on Aging at 2 or 18 months of age. Mice were allowed to acclimate for 1–2 weeks before treatment. During treatment mice were weighed 5 times per week, and control and experimental groups were housed in the same cage.

Exercise Treatment

Mice were separated into exercise groups based on arrival date at the facility. An 8-week forced swim regimen was used with up to 5 mice per tank. The water temperature was maintained at 35–37 °C at all times to minimize stress levels. Prior to the first week of swimming, the mice were acclimated to the tank with three 3-minute swimming sessions. Mice then swam 5 days per week for 10 minutes during the first week, 30 minutes per day for weeks 2–3, and 45 minutes per day for weeks 4–8. During treatments all mice were monitored for bobbing, “gang swimming,” or exhaustion, and they were dried after swimming.

Pulse wave velocity

PWV readings were recorded for each mouse before and after the exercise treatment. Mice were shaved on the abdomen and the upper back/neck regions a few days prior to ultrasound measurements. Mice were anesthetized with isoflurane, where the heart rate was maintained from 400–500 BPM, and the body temperature and ECG were constantly monitored. Doppler ultrasound was performed using a Vevo2100 with an MS550D transducer to measure transit time at abdominal and thoracic aorta locations. Abdominal readings were made with the animal supine and thoracic readings were made with the animal prone. Doppler readings with at least 5 heart beat cycles were recorded for each mouse 4–6 mm under the skin surface. The arrival time was calculated between the velocity upstroke and the peak of the R-wave and measured at thoracic and abdominal aorta locations. The transit time was calculated as the difference between the two arrival times as previously described (Williams *et al.*, 2007). PWV was calculated as the distance measured over the animal's body divided by the transit time.

Aorta preparation

Mice were anesthetized with 2–4% isoflurane until they were unresponsive. The chest cavity was then opened and the heart was perfused with 10 mL of phosphate buffered saline (PBS). The thoracic aorta was excised, cleaned of excess tissue, and stored in PBS on ice. Immediately prior to beginning AFM mechanical testing, the thoracic aorta was cut longitudinally, the ECs were scraped off as previously described (Peloquin *et al.*, 2011), and the tissue was bonded (Loctite Super Glue) to a petri dish and covered with room temperature PBS.

Atomic force microscopy

Contact mode AFM (Asylum MFP-3D) was used to measure subendothelial matrix elastic modulus of the thoracic aorta samples after ECs were removed. Measurements were taken in a 100 by 100 μm area of the artery in an 11x11 point grid with indents occurring every 10 μm . Indentations were made 300–500 nm into the tissue using a 5 μm radius spherical polystyrene bead on a silicon nitride cantilever with a spring constant of 0.12 N/m as calibrated by the manufacturer (Novascan Technologies). The AFM tips were calibrated before measuring each aorta sample and had a mean spring constant of 0.19 ± 0.03 N/m. The data was fit to the Hertz model assuming a Poisson's ratio of 0.5 (Peloquin *et al.*, 2011; Weisbrod *et al.*, 2013) using the Asylum curve fitting software to determine the elastic modulus.

Statistics

Group comparisons of the PWV data were conducted using the Student's t-test for normally distributed data and the Wilcoxon Rank-Sum test for non-normally distributed data, where normality was determined using a Shapiro-Wilk test (JMP software) with statistical significance at a p-value less than 0.05. Mean AFM data was analyzed using analysis of variance to compare more than two groups and the empirical cumulative distribution functions of the AFM data were compared pair-wise using the Kolmogorov-Smirnov test with p-values less than 0.05. To characterize the effects of age and exercise on arterial mechanics, and in particular the spatial heterogeneity of the elastic modulus maps, we estimated an additive model for the spatially-referenced elastic modulus measurements as a linear function of age and exercise, and a smooth (possibly non-linear) function of spatial location (Wood, 2006). The elastic modulus values were square-root-transformed to satisfy normality of the residuals. The additive model may be represented as a linear mixed effects model with the standard interpretation of the linear predictors, which in this case are group effects for age and exercise. The mouse-specific spatial effects terms were modeled using thin plate splines, which satisfy numerous optimality and smoothness properties, and are invariant to rotations of the spatial coordinate system. The model is a standard extension of a linear regression model, in which the spatial effects terms account for the spatial correlations of the elastic modulus map for each mouse, thereby permitting valid inference on the age and exercise effects. Computations were completed in R using the mgcv package (R Core Team, 2014).

The spatial heterogeneity of the elastic modulus maps was measured using the estimated smoothing parameters of the spatial effects terms. The spatial model may be cast as a linear mixed effects model in which the smoothing parameter corresponds to the inverse variance of a random effects term (Ruppert *et al.*, 2003), and therefore provides a natural, endogenous measure of spatial heterogeneity. For each estimated elastic modulus map, the smoothing parameter controls the balance between fidelity to the data and smoothness: large values encourage a smoother, more linear surface, while smaller values correspond to a rougher, interpolating surface. Compared with the sample variance of the data, the smoothing parameter provides a more direct measure of the spatial heterogeneity, since the sample variance does not distinguish between the variability of the surface and the measurement error. The smoothing parameters were log-transformed for computational stability and

outlier reduction, and the age and exercise group means of the log-smoothing parameters were computed. The sampling distribution of the log-smoothing parameter group means is not known, but can be estimated using the bootstrap (Efron and Tibshirani, 1994). The bootstrap re-sampling was performed at the mouse level to preserve the within-mouse spatial structures. Additional details on model fitting and bootstrapping are provided in the supplement.

Results

Mice were separated into treatment groups and showed no body weight change

Aged (18 months old at the beginning of the study) and young (2 months old at the beginning of the study) mice were used for age treatment groups, and the aged mice were separated into aged-sedentary (Aged Sed) and aged-exercised (Aged Ex) groups, which underwent a swimming regimen for 8 weeks (Fig. 1A). All mice were weighed 5 days per week to ensure stress on the animal is minimized as indicated by maintenance of a healthy weight (Fig. 1B).

Macro-scale arterial stiffening increases with age, decreases with exercise treatment, and is linearly correlated with subendothelial matrix elastic modulus

PWV is a measurement of bulk artery stiffness and is the standard clinical metric for predicting CVD (Mitchell *et al.*, 2010). Here, PWV measurements of male B6 mice were made using Doppler ultrasound and the transit time method, where the arrival time at each location was measured between peak of the R-wave on the ECG and the upstroke of the velocity profile (Fig. 2A) as previously described (Williams *et al.*, 2007). PWV measurements of young (2 months old) and aged (18 months old) mice taken before the exercise regimen indicate an increase in bulk arterial stiffness with age (Fig. 2B) as previously shown (Di Lascio *et al.*, 2014). Aged mice were divided into exercised and sedentary groups, and following an 8-week swimming exercise regimen, PWV was shown to decrease in aged mice (20 months old) compared to sedentary mice of the same age (Fig. 2C). These results demonstrate the prescribed exercise regimen described in Figure 1 cause changes in the bulk stiffness of arteries.

Micro-scale elastic modulus increases with age and decreases with exercise in aged mice

Although bulk stiffness of large arteries is assessed clinically, this information provides very little information about the mechanics of individual layers of the artery. Recent evidence from our lab and others has demonstrated that the mechanical environment of the intimal ECM dictates EC function and health (Huynh *et al.*, 2011; Kohn and Zhou *et al.*, 2015; Krishnan *et al.*, 2011; Stroka and Aranda-Espinoza, 2011a), underscoring the need to understand subendothelial matrix mechanics. Here, we used AFM coupled with a spherical probe and shallow indentations to produce force-distance curves analyzed using the Hertz model as previously described (Peloquin *et al.*, 2011). We validated the Hertz model in our system based on the goodness of fit, as shown in an example plot of the Hertz model fit to the data and the residuals of this fit (Fig. 3A). AFM was used to create elastic modulus maps of the subendothelial matrix along the thoracic aorta by profiling 100 by 100 μm tissue sections, from young (4 months old), aged-sedentary (20 months old), and aged-exercised

(20 months old) mice. This dimension was chosen because it is of sufficient size to provide the detail necessary to define the spatial distribution of elastic modulus beneath multiple cells in a monolayer. Average values across the grid indicate that subendothelial matrix elastic modulus increases with age and decreases with exercise in aged mice (Fig. 3B). The PWV measurements were plotted against the AFM results, indicating there is a positive and linear correlation between macro- and micro-scale elastic modulus (Fig. 3C).

Elastic modulus heterogeneity increases with age and decreases with exercise in aged mice

Typically, nano- and micro-indentation measurements of tissues have been reported as mean values (Figure 3B) (Engler *et al.*, 2004; Huynh *et al.*, 2011; Jacot *et al.*, 2006; Weisbrod *et al.*, 2013). However, most tissues, including the intima, are complex, and it is known that cells can respond to heterogeneous cues in matrix stiffness (Breckenridge *et al.*, 2014; Lo *et al.*, 2000). Using AFM, we probed the subendothelial matrix every 10 microns over a 100 by 100 micron space. Examination of the distribution of AFM values reveals that qualitative differences exist between the elastic modulus values in aged-sedentary (20 months old) mice compared to aged-exercised (20 months old) and young (4 months old) mice (Fig. 4A). The frequency of high elastic modulus values within the subendothelial matrix (above 50 kPa) is increased with age and decreased with exercise in aged mice (Fig. 4B). The empirical cumulative distribution functions of AFM elastic modulus values are changed with age and exercise in aged mice, demonstrating a larger spread of elastic modulus values in aged-sedentary mice compared to young mice or to aged-exercised mice (Fig. 4C). Overall, these data indicate that there is an increase in heterogeneity of mechanical elastic modulus values with age that can be reversed with exercise. These results suggest that the subendothelial matrix is more mechanically complex than previously thought.

Spatial micro-heterogeneities of elastic modulus increase with age and decrease with exercise

Our data indicate that there is an overall increase in the variations in mechanical measurements in the subendothelial matrix of aged-sedentary (20 months old) mice compared to young (4 months old) or aged-exercised (20 months old) mice (Figure 4). To investigate the spatial dependence of these heterogeneities, we examined the distribution of elastic modulus values taken every 10 μm over a 100 by 100 μm area. Spatial heterogeneity profiles of aortic subendothelial matrix demonstrate complex patterns of elastic modulus ‘hotspots’ in the aged-sedentary mice (Fig. 5A). To determine how the locations of elastic modulus ‘hotspots’ varied between experimental cohorts, we employed a linear mixed effects model. The linear mixed effects model with mouse-specific spatial effects was estimated from the square-root-transformed elastic modulus data, which satisfies normality of the residuals. The sampling distributions of the group differences in log-smoothing parameters were estimated using 1,000 bootstrap simulations. Among sedentary mice, the log-smoothing parameters were lower for aged-sedentary mice than young mice in 95% of the bootstrap simulations (Fig. 5B). Among aged mice, the log-smoothing parameters were lower for sedentary mice in 92% of the bootstrap simulations than for the aged-exercised mice (Fig. 5C). Together these data indicate that the model predicts that spatial heterogeneity increases with age and decreases with exercise in aged mice.

Discussion

Here, we show that the elastic modulus profiles of the mouse aortic subendothelial matrix are more complex than previously reported, and this complexity is a function of age and exercise. The elastic modulus measured using an AFM within a 100 μm by 100 μm patch can vary from 2 to 100 kPa. Heterogeneity in elastic modulus increases with age and decreases with exercise, and importantly, the spatial variation of these values also follows the same trend. These data indicate that aged-sedentary mice contain subendothelial matrix profiles that are more mechanically complex than those of young or aged-exercised mice. Our data also indicate that the increase of mean micro-scale elastic modulus with age and decrease with exercise correlates with macro-scale PWV measurements. PWV measures the bulk artery stiffness, which is thought to be influenced in most part by the thick medial layer (Kohn and Lampi *et al.*, 2015; Shadwick, 1999). This measurement does not account for the complexities of mechanical micro-heterogeneities found using AFM. Our data indicate that PWV, the current gold standard clinical technique, may also give an indication of mean micro-scale intimal health.

Arterial stiffness has been shown to increase with increased collagen deposition, the degradation of elastin fibers, and the action of crosslinking agents such as advanced glycation end products (AGEs) (Fleenor *et al.*, 2012; Greenwald, 2007; Kohn and Lampi *et al.*, 2015). Collagen is a major contributor to the mechanical properties of the artery, and the increased presence of collagen fibers in the artery over elastin fibers contributes to bulk arterial stiffening (Díez, 2014; Fleenor and Berrones, 2015). As arteries age, collagen production increases and elastin content decreases, leading to an increase in overall arterial stiffness (Gu *et al.*, 2014a; Kohn and Lampi *et al.*, 2015; Ziemann *et al.*, 2005). Exercise has the opposite effect on arterial composition, resulting in more compliant vessels (Gu *et al.*, 2014a). Increased stiffness in arteries from aged mice is also likely partly due to the increased presence of ECM cross-linkers such as AGEs (Fleenor *et al.*, 2012), which are mitigated with exercise (Gu *et al.*, 2014b). The underlying causes of increased mechanical heterogeneities describe in our study are not yet clear. It is possible that they are due to increased collagen aggregation (Greenberg, 1986; Keyes *et al.*, 2011) and/or changes in collagen cross-linking. While artery fiber composition has been studied in relation to age and exercise (Avolio *et al.*, 1998; Gu *et al.*, 2014a; Schlatmann and Becker, 1977), less is known about specific micro-scale changes in the subendothelial matrix at the scale at which AFM is detecting. Further studies are required to determine the specific physical and biochemical changes which cause the increase in heterogeneity we report here.

PWV is the gold standard for measuring macro-scale artery stiffness due to its clinical accessibility and application as a strong predictor of CVD (Kohn and Lampi *et al.*, 2015; Laurent *et al.*, 2006; Van Bortel *et al.*, 2012). High aortic PWV in humans is associated with a 48% increase in CVD risk (Mitchell *et al.*, 2010). Our data confirm reports from others indicating PWV increases with age and decrease with exercise in rodents (Di Lascio *et al.*, 2014; Gu *et al.*, 2014a). Ours is the first study to our knowledge to show that macro- and micro-scale stiffness measurements in the artery are linearly correlated. Together with our previous data demonstrating that matrix stiffness can induce EC dysfunction (Huynh *et al.*, 2011; Kohn and Zhou *et al.*, 2015), these data suggest that that clinical evaluation of the

artery using PWV could provide information about subendothelial matrix mechanics and EC health. The assessment of subendothelial matrix and EC function using macro-scale techniques may allow for new insights into cardiovascular health and the relationship between arterial stiffness and disease progression.

Based on our data, the elastic modulus of the subendothelial matrix can range over an order of magnitude, indicating that ECs experience a non-uniform, complex mechanical environment *in vivo*. It is well known that ECs respond to the mechanical properties of their matrix (Hsu *et al.*, 2015; Kohn and Lampi *et al.*, 2015; Kohn and Zhou *et al.*, 2015; Stroka and Aranda-Espinoza, 2011a). Matrix stiffness can regulate EC traction forces, contractility, and F-actin stress fiber formation through Rho/ROCK/MLCK signaling (Birukova *et al.*, 2013; Hsu *et al.*, 2015; Huynh *et al.*, 2011; Ridley, 2001; Stroka and Aranda-Espinoza, 2011a; Szulcek *et al.*, 2013). AFM elastic modulus maps described here indicate that aged-sedentary mice have more heterogeneous elastic modulus profiles. Recently, single cell studies have demonstrated that cells exert heterogeneous traction forces in response to a heterogeneous ECM (Breckenridge *et al.*, 2014). Importantly, higher cellular traction forces have been shown to result in centripetal cellular tension that disrupts EC-EC contacts, causing the formation of gaps in the EC monolayer (Huynh *et al.*, 2011; Krishnan *et al.*, 2011; Stroka and Aranda-Espinoza, 2011b). Given the known role of matrix stiffness in the regulation of cellular traction forces and the role of traction force in preserving monolayer integrity, it is likely that more complex mechanical elastic modulus profiles like those we describe here may result in increased disruption of barrier function with age. Our results underscore the need for the development of novel *in vitro* platforms that accurately reflect the micro-heterogeneities in elastic modulus present in the subendothelial matrix and a need to better understand how cells integrate multiple mechanical cues.

Supplementary Material

Refer to Web version on PubMed Central for supplementary material.

Acknowledgments

We gratefully acknowledge help and support from Dr. Christopher Umbach for AFM support and from Dr. Rebecca Williams and Dr. Johanna Dela Cruz for ultrasound assistance. This work made use of the Cornell Center for Materials Research Shared Facilities which are supported through the NSF MRSEC program (DMR-1120296). High-resolution sonography was carried out in the Cornell University Biotechnology Resource Center, with NIH S10OD016191 funding for the shared VisualSonics high-resolution ultrasound. This work was supported from grants from the National Science Foundation (award number 1435755), and the National Institutes of Health to C.A.R (project number 1R01HL127499-01), and a Graduate Research Fellowship Program to J.C.K. (2013165170) under Cornell University NSF grant DGE-1144153.

Notation

CVD	cardiovascular disease
PWV	pulse wave velocity
AFM	atomic force microscopy
EC	endothelial cell

Aged Sed	aged sedentary mice
Aged Ex	aged exercised mice
ECM	extracellular matrix

References

- Avolio A, Jones D, Tafazzoli-Shadpour M. Quantification of alterations in structure and function of elastin in the arterial media. *Hypertension*. 1998; 32:170–175. [PubMed: 9674656]
- Birukova AA, Tian X, Cokic I, Beckham Y, Gardel M, Birukov KG. Endothelial barrier disruption and recovery is controlled by substrate stiffness. *Microvascular Research*. 2013; 87:50–57. [PubMed: 23296034]
- Breckenridge MT, Desai RA, Yang MT, Fu J, Chen CS. Substrates with engineered step changes in rigidity induce traction force polarity and durotaxis. *Cell and Molecular Bioengineering*. 2014; 7:26–34.
- Díez, J. Structural Alterations in Arterial Stiffness: Role of Arterial Fibrosis. In: Safar, M.; O'Rourke, E.; Frohlich, E., editors. *Blood Pressure and Arterial Wall Mechanics in Cardiovascular Diseases*. Springer-Verlag; London: 2014. p. 205-214.
- Di Lascio N, Stea F, Kusmic C, Sicari R, Fatta F. Non-invasive assessment of pulse wave velocity in mice by means of ultrasound images. *Atherosclerosis*. 2014; 237:31–37. [PubMed: 25194332]
- Efron, B.; Tibshirani, RJ. *An introduction to the bootstrap*. CRC Press; New York: 1994.
- Engler AJ, Richert L, Wong JY, Picart C, Discher DE. Surface probe measurements of the elasticity of sectioned tissue, thin gels and polyelectrolyte multilayer films: Correlations between substrate stiffness and cell adhesion. *Surface Science*. 2004; 570:142–154.
- Fleenor, BS.; Berrones, AJ. *Arterial Stiffness: Implications and Interventions*. Springer International Publishing; New York: 2015. *Structural Changes Contributing to Arterial Stiffness: Compositional Changes*; p. 19-20.
- Fleenor BS, Sindler AL, Eng JS, Nair DP, Dodson RB, Seals DR. Sodium nitrite de-stiffening of large elastic arteries with aging: Role of normalization of advanced glycation end-products. *Experimental Gerontology*. 2012; 29:997–1003.
- Greenberg SR. The association of medial collagenous tissue with atheroma formation in the aging human aorta as revealed by a special technique. *Histology and Histopathology*. 1986; 1:323–326. [PubMed: 2980126]
- Greenwald SE. Ageing of the conduit arteries. *Journal of Pathology*. 2007; 211:157–172. [PubMed: 17200940]
- Grundy SM, Pasternak R, Greenland P, Smith S, Fuster V. Assessment of cardiovascular risk by use of multiple-risk-factor assessment equations. *Circulation*. 1999; 100:1481–1492. [PubMed: 10500053]
- Gu Q, Wang B, Zhang XF, Ma YP, Liu JD, Wang XZ. Chronic aerobic exercise training attenuates aortic stiffening and endothelial dysfunction through preserving aortic mitochondrial function in aged rats. *Experimental Gerontology*. 2014a; 56:37–44. [PubMed: 24607516]
- Gu Q, Wang B, Zhang XF, Ma YP, Liu JD, Wang XZ. Contribution of receptor for advanced glycation end products to vasculature-protecting effects of exercise training in aged rats. *European Journal of Pharmacology*. 2014b; 741:186–194. [PubMed: 25160740]
- Hsu BY, Bae YH, Mui KL, Liu S-L, Assoian RK. Apolipoprotein E3 inhibits Rho to regulate the mechanosensitive expression of Cox2. *Public Library of Science One*. 2015:10.
- Huynh J, Nishimura N, Rana K, Peloquin JM, Califano JP, Montague CR, King MR, Schaffer CB, Reinhart-King CA. Age-related intimal stiffening enhances endothelial permeability and leukocyte transmigration. *Science Translational Medicine*. 2011; 3:112–122.
- Jacot JG, Dianis S, Schnall J, Wong JY. A simple microindentation technique for mapping the microscale compliance of soft hydrated materials and tissues. *Journal of Biomedical Materials Research Part A*. 2006; 79A:485–494. [PubMed: 16779854]

- Keyes JT, Haskett DG, Utzinger U, Azhar M, Vande Geest JP. Adaptation of a planar microbiaxial optomechanical device for the tubular biaxial microstructural and macroscopic characterization of small vascular tissues. *Journal of Biomechanical Engineering*. 2011;133.
- Klein EA, Yin L, Kothapalli D, Castagnino P, Byfield FJ, Xu T, Levental I, Hawthorne E, Janmey PA, Assoian RK. Cell-cycle control by physiological matrix elasticity and in vivo tissue stiffening. *Current Biology*. 2009; 19:1511–8. [PubMed: 19765988]
- Kohn JC, Lampi MC, Reinhart-King CA. Age-related vascular stiffening: causes and consequences. *Frontiers Genetics*. 2015; 6:1–17.
- Kohn JC, Zhou DW, Bordeleau F, Zhou AL, Mason BN, Mitchell MJ, King MR, Reinhart-King CA. Cooperative effects of matrix stiffness and fluid shear stress on endothelial cell behavior. *Biophysical Journal*. 2015; 108:471–478. [PubMed: 25650915]
- Krishnan R, Klumpers DD, Park CY, Rajendran K, Trepas X, van Bezu J, van Hinsbergh VWM, Carmen CV, Brain JD, Fredberg JJ, Butler JP, van Nieuw Amerongen GP. Substrate stiffening promotes endothelial monolayer disruption through enhanced physical forces. *American Journal of Physiology: Cell Physiology*. 2011; 300:C146–C154. [PubMed: 20861463]
- Laurent S, Cockcroft J, Van Bortel L, Boutouyrie P, Giannattasio C, Hayoz D, Pannier B, Vlachopoulos C, Wilkinson I, Struijker-Boudier H. Expert consensus document on arterial stiffness: Methodological issues and clinical applications. *European Heart Journal*. 2006; 27:2588–2605. [PubMed: 17000623]
- Lo CM, Want HB, Dembo M, Wang YL. Cell movement is guided by the rigidity of the substrate. *Biophysical Journal*. 2000; 79:144–152. [PubMed: 10866943]
- Millonig G, Niederegger H, Wick G. Analysis of the cellular composition of the arterial intima with modified en face techniques. *Laboratory Investigation*. 2001; 81:639–641. [PubMed: 11304584]
- Mitchell GF, Vasan RS, Larson G, Pencina MJ, Hamburg NM, Vita JA, Levy D, Benjamin EJ. Arterial stiffness and cardiovascular events: the Framingham Heart Study. *Circulation*. 2010; 121:505–511. [PubMed: 20083680]
- Peloquin J, Huynh J, Williams RM, Reinhart-King CA. Indentation measurements of the subendothelial matrix in bovine carotid arteries. *Journal of Biomechanics*. 2011; 44:815–821. [PubMed: 21288524]
- R Core Team. R: A language and environment for statistical computing. R Foundation for Statistical Computing; Vienna, Austria: 2014. <http://www.R-project.org/>
- Ridley A. Rho family proteins: Coordinating Cell Responses. *Trends in Cell Biology*. 2001; 11:471–477. [PubMed: 11719051]
- Ruppert, D.; Wand, MP.; Carroll, RJ. *Cambridge Series in Statistical and Probabilistic Mathematics*. Cambridge University Press; 2003. Semiparametric regression.
- Schlatmann TJM, Becker AE. Histologic changes in the normal aging aorta: Implications for dissecting aortic aneurysm. *The American Journal of Cardiology*. 1977; 39:13–20. [PubMed: 831420]
- Shadwick RE. Mechanical design in arteries. *The Journal of Experimental Biology*. 1999; 202:3305–3313. [PubMed: 10562513]
- Steppan J, Sikka G, Jandu S, Barodka V, Halushka MK, Flavahan NA, Belkin AM, Nyhan D, Butlin M, Avolio A, Berkowitz DE, Santhanam L. Exercise, vascular stiffness, and tissue transglutaminase. *Journal of the American Heart Association*. 2014; 3:1–11.
- Stroka KM, Aranda-Espinoza H. Endothelial cell substrate stiffness influences neutrophil transmigration via myosin light chain kinase-dependent cell contraction. *Blood*. 2011a; 118:1632–1640. [PubMed: 21652678]
- Stroka KM, Aranda-Espinoza H. Effects of morphology vs. cell–cell interactions on endothelial cell stiffness. *Cell and Molecular Bioengineering*. 2011b; 4:9–27.
- Stroka KM, Levitan I, Aranda-Espinoza H. OxLDL and substrate stiffness promote neutrophil transmigration by enhanced endothelial cell contractility and ICAM-1. *Journal of Biomechanics*. 2012; 45:1828–1834. [PubMed: 22560286]
- Szulcek R, Beckers CML, Hodzic J, de Wit J, Chen Z, Grob T, Musters RJP, Minshall RD, van Hinsbergh VWM, van Nieuw Amerongen GP. Localized RhoA GTPase activity regulates

dynamics of endothelial monolayer integrity. *Cardiovascular Research*. 2013; 99:471–82. [PubMed: 23536606]

- Tanaka H, Dinunno FA, Monahan KD, Clevenger CM, DeSouza CA, Seals DR. Aging, habitual exercise, and dynamic arterial compliance. *Circulation*. 2000; 102:1270–1275. [PubMed: 10982542]
- Van Bortel LM, Laurent S, Boutouyrie P, Chowienczyk P, Cruickshank JK, De Backer T, Filipovsky J, Huybrechts S, Mattace-Raso FU, Protogerou AD, Schillaci G, Segers P, Vermeersch S, Weber T. Expert consensus document on the measurement of aortic stiffness in daily practice using carotid-femoral pulse wave velocity. *Journal of Hypertension*. 2012; 30:445–448. [PubMed: 22278144]
- Wang YL, Pelham RJ. Preparation of a flexible, porous polyacrylamide substrate for mechanical studies of cultured cells. *Methods in Enzymology*. 1998; 298:489–496. [PubMed: 9751904]
- Weisbrod RM, Shiang T, Al Sayah L, Fry JL, Bajpai S, Reinhart-King CA, Lob HE, Santhanam L, Mitchell G, Cohen RA, Seta F. Arterial stiffening precedes systolic hypertension in diet-induced obesity. *Hypertension*. 2013; 62:1105–10. [PubMed: 24060894]
- Williams R, Needles A, Cherin E, Zhou YQ, Henkelman RM, Adamson SL, Foster FS. Noninvasive ultrasonic measurement of regional and local pulse-wave velocity in mice. *Ultrasound in Medicine and Biology*. 2007; 33:1368–1375. [PubMed: 17561330]
- Wood, SN. *Generalized additive models: and introduction with R*. Chapman & Hall/CRC; Boca Raton: 2006.
- Zieman SJ, Melenovsky V, Kass DA. Mechanisms, pathophysiology, and therapy of arterial stiffness. *Arteriosclerosis, Thrombosis, and Vascular Biology*. 2005; 25:932–43.

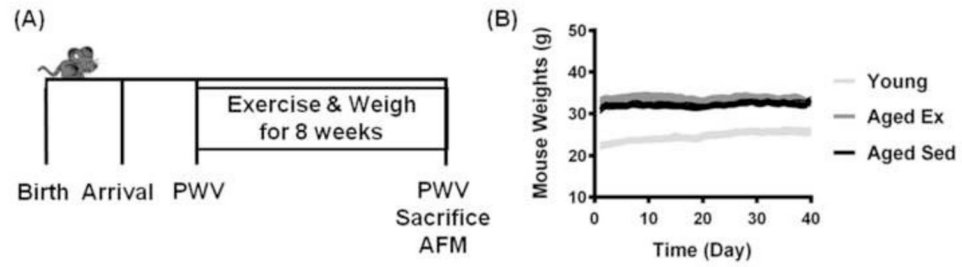


Figure 1. Schematic of timeline of experimental procedures. (A) Mice were received at Cornell, and given time to acclimate prior to the exercise regimen. PWV measurements were taken before and after exercise. AFM measurements were taken after sacrifice. (B) Weights of mice throughout the experimental timeline. Lines represent mean and SEM.

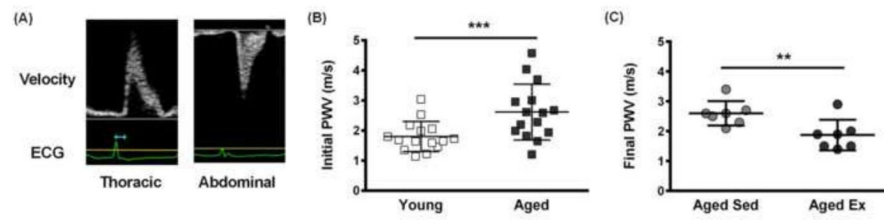


Figure 2.

Macro-scale stiffness increases with age and decreases with exercise. (A) Representative Doppler ultrasound images used to measure the transit time between the thoracic and abdominal aorta. The arrival times at each location are shown in blue. (B) PWV measurements in aged mice (18 months old, $n=15$ mice) relative to young mice (2 months old, $n=14$ mice), *** $p<0.005$ (Student's t-test). (C) PWV measurements in aged-sedentary mice (20 months old, $n=7$ mice) and aged-exercised mice (20 months old, $n=7$ mice) taken after an exercise regimen performed by half of the aged mice, ** $p<0.02$ (Wilcoxon-Rank Sum test).

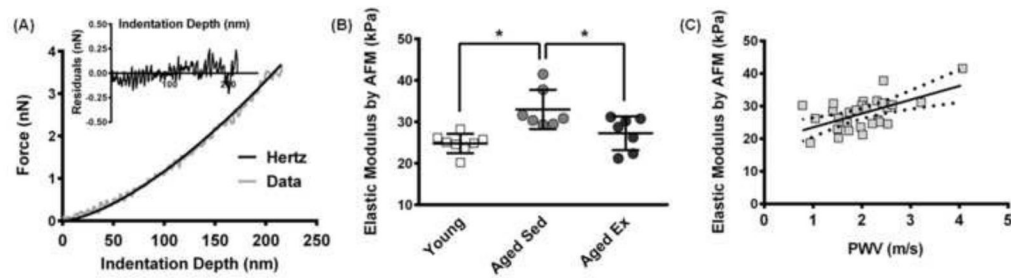


Figure 3.

Micro-scale elastic modulus increases with age and decreases with exercise. (A) Representative Hertz model fit to AFM force-indentation curve, and inset shows the residuals of the Hertz model fit to the data. (B) The mean elastic modulus of the subendothelial matrix in aged-sedentary mice (20 months old, $n=7$ mice) relative to young mice (4 months old, $n=8$ mice) and aged-exercised mice (20 months old, $n=7$ mice) based on AFM measurements, * $p<0.01$ (Linear Mixed Effects Model, square-root transform). (C) Comparison of PWV macro-scale stiffness with micro-scale AFM elastic modulus values from each mouse, $p<0.02$ (Linear Mixed Effects Model). The solid line indicates the linear fit and the dotted lines indicate the standard error.

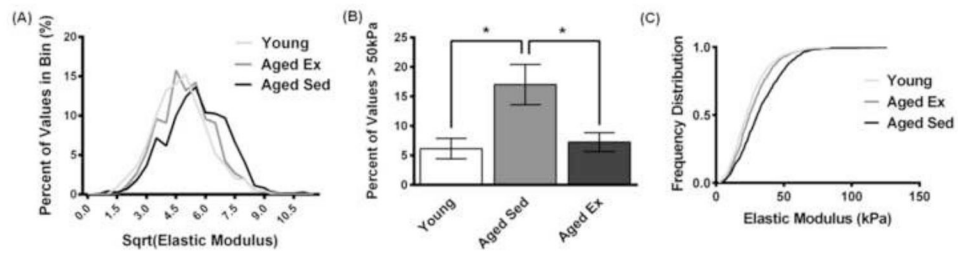


Figure 4.

Range of AFM elastic modulus values increases with age and decreases with exercise. (A) Representative stiffness heterogeneity profiles of the aortic intima demonstrate heterogeneous distributions where young and aged-exercised mice have a more positive skew (square-root transform). (B) Plot of AFM measurement values greater than 50 kPa in aged-sedentary mice compared to young and aged-exercised mice, * $p < 0.05$ (ANOVA), error bars SEM. (C) The empirical cumulative distribution functions of the spread of values of the aged-sedentary mice compared to both the young and the aged-exercised mice ($p < 0.0001$, pairwise comparisons using the Kolmogorov-Smirnov test).

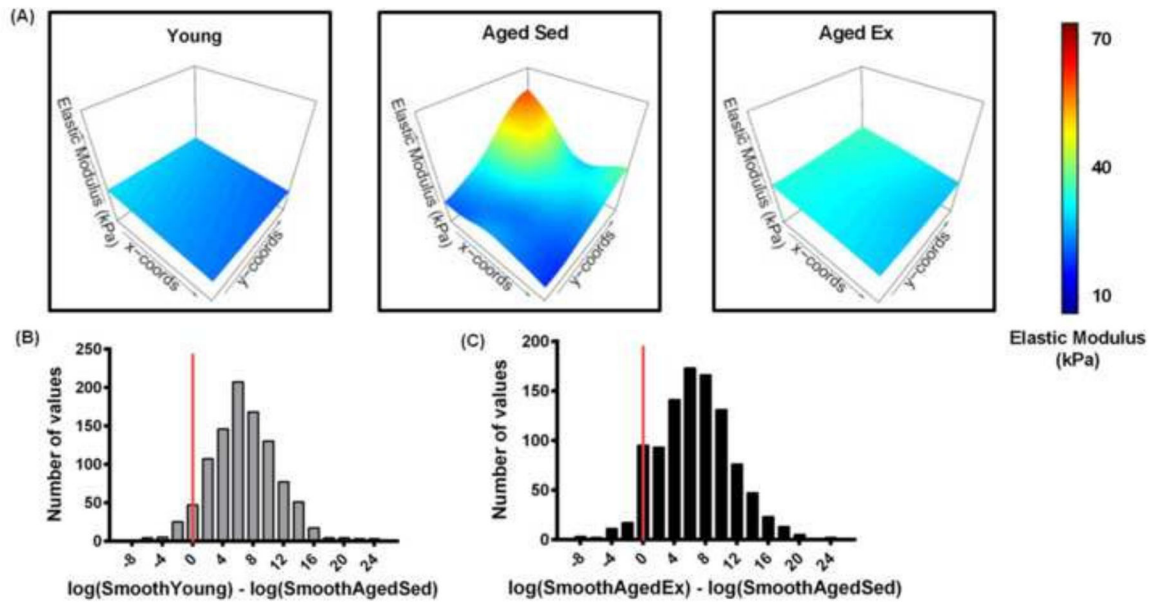


Figure 5.

The spatial heterogeneity of elastic modulus values in the mouse aorta increases with age and decreases with exercise. (A) Representative AFM elastic modulus maps of a 100 by 100 μm aorta sections demonstrating ‘hotspots’ of increased elastic modulus in the aged-sedentary mice and complex spatial patterns of increased elastic modulus. Histograms of bootstrap simulations of the smoothing parameter for the AFM measurements of the (B) aged-sedentary mice compared to young mice, and (C) aged-sedentary mice compared to aged-exercised mice (Linear Mixed Effects Model, log transform) indicate that the spatial heterogeneity of subendothelial matrix stiffness increases with age and decreases with exercise in aged mice. Data to the right of the red line indicate simulations where the aged-sedentary mice have more spatial heterogeneity than the compared group.